ACADEMIC PRESS

Bioorganic Chemistry 30 (2002) 264–275

BIOORGANIC CHEMISTRY

www.academicpress.com

pH Dependence of inhibitors targeting the occluding loop of cathepsin B

Brian E. Cathers,*[,1] Cynthia Barrett, James T. Palmer, and Robert M. Rydzewski

Axys Pharmaceuticals Inc., 180 Kimball Way, South San Francisco, CA 94080, USA

Received 1 November 2001

Abstract

Potent and selective cathepsin B inhibitors have previously been synthesized based upon the natural product cysteine protease inhibitor E-64. X-ray crystal data indicates that these compounds interact through their free carboxylate with the positively charged histidine residues located on the prime-side of the active site within the occluding loop of cathepsin B. Herein, we examine the pH dependence of two prime-side-binding compounds. In each case there is a dramatic decrease in k_{inact}/K_I as the pH is raised from 4 to 7.8 corresponding to a single ionization of pK_a 4.4. These results suggest that targeting of the occluding loop of cathepsin B may be a poor inhibitor design strategy if the enzyme environment has a pH greater than 5.5. However, this type of inhibitor may be a useful tool to help elucidate the role and the environment of cathepsin B in invading tumors. © 2002 Elsevier Science (USA). All rights reserved.

Keywords: Cathepsin B; CA-074; Occluding loop; pH; Inhibitor; E-64; Cancer

* Corresponding author. Fax: 1-858-793-5648.
E-mail address: bcathers@newbiotics.com (B.E. Cathers).
[1] Present address: NewBiotics, Inc., 4939 Directors Place, San Diego, CA 92121, USA.

0045-2068/02/$ - see front matter © 2002 Elsevier Science (USA). All rights reserved.
PII: S0045-2068(02)00009-3

1. Introduction

Cathepsin B is one of the most widely studied members of the papain superfamily of cysteine proteases. Typical for this family, cathepsin B is synthesized as an inactive zymogen, and the enzyme is activated at acidic pH by autoproteolysis [1]. However, unlike other members of the papain family, which are mostly endo-proteases, cathepsin B displays both exo- and endo-proteolytic activities [2,3]. The characteristic feature of the cathepsin B structure that imparts the exo-proteolytic activity is an 18 amino acid residue insertion that "occludes" substrates from the prime side of the binding pocket, and through two critical residues (His 110 and His 111), provides the requisite positive charge for binding the negatively charged C-terminal carboxylate of exo-substrates [4]. Mutagenesis and pH studies have demonstrated that the "occluding loop" is a hydrogen ion-dependent gate for controlling not only the type of proteolysis (exo- or endo-) but also for controlling the maturation of the pro-enzyme [5–7]. At neutral pH the occluding loop is found displaced from the prime-side-binding cleft by the pro-region of the immature polypeptide. At low pH, the occluding loop is thought to displace the pro-region peptide making it available for proteolysis. Once activated, cathepsin B acts as an exo-protease at low pH (occluding loop bound in the prime-side of the active site cleft) and an endo-protease at neutral pH.

Cathepsin B has been implicated in many disease states including cancer progression and metastasis [8–14]; however, a causal relationship has yet to be definitively established. One reason is the lack of potent and selective cathepsin B inhibitors. A strategy for producing a truly specific cathepsin B inhibitor is to take advantage of the unusual feature of cathepsin B that distinguishes it from most other cathepsins in the papain superfamily, namely the occluding loop. Based on the crystal structure published by Musil et al. [4], the structure of the natural product cathepsin inhibitor E-64 was modified to take advantage of the occluding loop

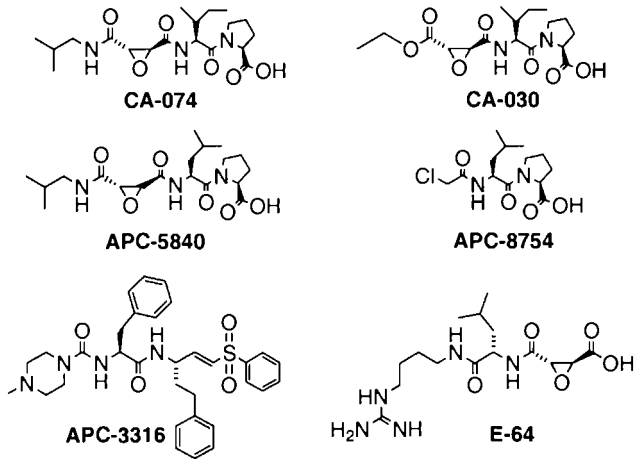

Fig. 1. Cathepsin B inactivators. The structures of the known occluding-loop binding inhibitors CA-074 and CA-030 are shown for comparison.

contacts found in cathepsin B [15,16]. The most potent analogue from this series, CA-074 (Fig. 1), was found to be a very specific inhibitor of cathepsin B. Recently, Linebaugh et al. [17] reported a 10-fold decrease in potency of CA-074 at pH 7.0 compared with pH 6.0, and prior to that, Schaschke et al. [18] demonstrated the pH dependence of the inhibitory activity of CA-074 analogues over the pH range of 5.5–7.5. They also noted the relative pH independence of E-64 over that same pH range. Herein, we examine in greater detail the pH-dependent inactivation of cathepsin B by E-64 and two analogues of CA-074 (Fig. 1) and conclude that occluding loop gating of endo- to exo-proteolysis occurs with a pK_a of 4.4 not 5.5 as previously reported [2]. These results also suggest that inhibitors designed to interact with the occluding loop will be most effective at low pH.

2. Materials and methods

Human liver cathepsin B was obtained from Athens Research and Technology (Athens, GA). The substrate, Boc-Leu–Lys–Arg-AMC was purchased from Bachem. E-64 was purchased from Sigma. All other reagents used were of highest quality and purity available. Data analysis was performed by use of the program GraFit (Erithacus Software).

2.1. Synthesis of inhibitors

APC-5840 (i-BuNH-EpsLeuPro-OH) was synthesized as previously described [19].

N-(Chloroacetyl)-leucylproline tert-butyl ester. Leucylproline *tert*-butyl ester [18] (430 mg, 1.51 mmol) was dissolved in dichloromethane (20 mL), and the solution was stirred with 1 M sodium carbonate (10 mL). Chloroacetyl chloride (0.13 mL, 1.59 mmol) was added to the mixture with vigourous stirring. After 15 min, stirring was discontinued and the organic phase was separated, washed with water and brine, and dried over magnesium sulfate. Filtration and solvent evaporation gave an off-white solid. This was recrystallized from ethyl acetate/hexane to afford 325 mg of *N*-(chloroacetyl)-leucylproline *tert*-butyl ester as colorless needles, m.p. 121–123 °C (a 60% yield). ^{1}H NMR (300 MHz, DMSO-d$_6$): δ 8.50 (d, $J = 8$ Hz, 1H), 4.53 (m, 1H), 4.15 (m, 1H), 4.05 (ABq, 2H), 3.65 (m, 1H), 3.46 (m, 1H), 2.14 (m, 1H), 1.40–1.95 (m, 6H), 1.35 (s, 9H), 0.87 (d, 6H). LCMS (APCI): mH^+ 361 (100%).

APC-8754 ((ClCH$_2$CO)LeuPro-OH). *N*-(Chloroacetyl)-leucylproline *tert*-butyl ester (201 mg, 0.56 mmol) was dissolved in dichloromethane (2.0 mL), and trifluoroacetic acid (8 mL) was added. The solution was stirred at ambient temperature for 1 h. Evaporation of the solvent followed by vacuum drying of the residue afforded 170 mg of APC-8754 (a 100% yield) as a pale yellow oil. ^{1}H NMR (300 MHz, DMSO-d$_6$): δ 8.47 (d, $J = 8$ Hz, 1H), 4.53 (m, 1H), 4.22 (m, 1H), 4.05 (ABq, 2H), 3.4–3.7 (m, 2H), 2.12 (m, 1H), 1.75–1.97 (m, 3H), 1.60 (m, 1H), 1.44 (m, 2H), 0.86 (m, 6H). LCMS (APCI): mH^+ 305 (100%).

(S)-Benzyl-2-[(4-methylpiperazine-1-carbonyl)-amino]-3-phenylpropionate (Me-Pip-PheOBzl). To a solution of (*S*)-benzyl-2-isocyanato-3-phenylpropionate

(OCN-PheOBzl) [20] (45.86 g, 163 mmol) in THF (250 mL) at 0 °C was added *N*-methylpiperazine (18.08 mL, 163 mmol). The mixture was stirred for 30 min and was concentrated in vacuo to a pale orange oil that crystallized on standing. MePip-PheOBzl (theoretical yield 62.19 g) was used without further purification.

(S)-2-[(4-Methyl-piperazine-1-carbonyl)-amino]-3-phenylpropionic acid (MePip-PheOH). A solution of MePip-PheOBzl (62.19 g, 163 mmol) in ethanol (400 mL) was charged with 10% palladium on active charcoal (4.5 g). The solution was exposed to hydrogen on a Parr shaker (30 psi) for 6 h, filtered through Celite, and concentrated in vacuo. The residue was triturated with ether (700 mL) to remove residual ethanol, and was reprecipitated from CH_2Cl_2/ether to give 44.31 g (93%) MePip-PheOH. ^{1}H NMR (d^6-DMSO): δ 2.15 (3H, s); 2.18 (4H, m); 2.84–2.94 (1H, dd, $J = 15$, 11 Hz); 2.95–3.04 (1H, dd, $J = 15$, 5 Hz); 3.14–3.30 (4H, m); 4.17 (1H, m); 6.65 (1H, d, $J = 8$ Hz); 7.17–7.27 (5H, m).

APC-3316 tosylate. A 2-L, 3-necked round bottomed flask equipped with an overhead stirrer, a thermometer, and an addition funnel was charged with a solution of MePip-PheOH (44.3 g, 152 mmol) in 3:1 THF/DMF (400 mL). The mixture was cooled to −10 °C, whereupon 4-methylmorpholine (16.72 mL, 152 mmol) was added, followed by a solution of isobutyl chloroformate in THF (50 mL) over 20 min, with vigorous stirring. The temperature was maintained at or below −5 °C throughout the addition. The mixture was stirred for 1 h. 3-Benzenesulfonyl-1-phenethylallylamine tosylate (TsOH.HphVSPh) [21] (72.0 g, 152 mmol) was added as a solid. 4-Methylmorpholine (16.72 mL, 152 mmol) was added dropwise, careful temperature control being maintained between −5 and −10 °C to minimize epimerization of the phenylalanine residue. The mixture was stirred for 1 h. Saturated aqueous $NaHCO_3$ (500 mL) was added. The mixture was extracted with ethyl acetate (600 mL), washed with brine, dried over $MgSO_4$, filtered, and concentrated. The thick oily residue was dissolved in acetonitrile (200 mL) and was added to a solution of *p*-toluenesulfonic acid monohydrate (28.91 g, 152 mmol) in acetonitrile (300 mL). The solution was allowed to stand overnight following addition of a small seed crystal. The product was filtered, washed with ether (2 × 300 mL), air dried, and recrystallized from hot acetonitrile to give 70.29 g (62%) of APC-3316 tosylate.

APC-3316 hydrochloride (MePip-Phe-HphVSPh · HCl). Acetonitrile (800 mL) was added to APC-3316 tosylate (173.4 g, 0.232 mol from multiple combined batches). The mixture was heated on a hot plate/stirrer until all the solids had dissolved. The solution was allowed to cool to room temperature and stand for 48 h. The solids were filtered, washed with acetonitrile (1 L) and ether, and were air-dried. The pure tosylate was partitioned between saturated aqueous $NaHCO_3$ (1 L) and ethyl acetate (800 mL), and the organic layer was washed with brine (500 mL), dried over $MgSO_4$, filtered, and concentrated to a total weight of 154 g (APC-3316 free base plus solvent). This material was dissolved in CH_2Cl_2 (400 mL) and was added dropwise over 3 h to a vigorously stirred solution of 1.0 M hydrogen chloride in ether (460 mL) then diluted with 4 L of dry ether. The solids were stirred for an additional 12 h, filtered, washed with ether (4 × 1 L), hexane (3 × 1 L) and dried to constant weight at 45 °C under vacuum. The yield of APC-3316 hydrochloride was 134 g (94% from the tosylate, 34% total yield from commercially available materials). ^{1}H NMR (d^6-DMSO): δ 1.8 (1H, m); 1.9 (1H, m); 2.49–2.9 (4H, m*); 2.7 (3H, d, $J = 4$ Hz); 2.95

(2H, m*); 3.04–3.26 (2H, m*); 3.35 (2H, d, $J = 11$ Hz); 4.03–4.17 (2H, m); 4.32 (1H, m); 4/48 (1H, m); 6.52 (1H, d, $J = 15$ Hz); 6.87 (1H, dd, $J = 15, 4$ Hz); 7.13–7.31 (10H, m); 7.61–7.74 (3H, m); 7.85 (2H, d, $J = 8$ Hz); 8.44 (1H, d, $J = 8$ Hz); 11.30 (1H, br. s). ^{13}C NMR (d^6-DMSO); 32.0, 35.3, 37.9, 41.3, 42.5, 49.3, 52.5, 52.6, 57.4, 126.4, 127.7, 128.6, 128.8, 129.0, 129.8, 130.2, 134.2, 138.8, 140.9, 141.8, 147.9, 157.3, 172.8. MS (M^{+1}): 575 (signal of free base).

Enzymatic assays. Typical assay buffer ranging in pH from 4.0 to 7.8 contained 50 mM each of sodium acetate, MES, and sodium phosphate plus 2.5 mM EDTA, 2.5 mM DTT (added fresh on the day of use), and 0.001% Tween 20. All experiments were conducted at room temperature. DMSO (10% final v/v) was used in all assays to increase inhibitor solubility or simply as a control. Hydrolysis of the substrate Boc-Leu–Lys–Arg-AMC was monitored in a continuous fashion by use of a Molecular Devices fmax plate reader (filter pair: excitation 355, emission 460 nm). The kinetic parameters k_{cat} and K_m were determined over the pH range listed above using a response factor of 275 RFU/μM AMC (determined experimentally under the same assay conditions with pure AMC stock solutions). The response factor was insensitive to changes in pH. Inactivation of cathepsin B (1.1 nM final concentration) was monitored continuously as above in the presence of 300 μM Boc-Leu–Lys–Arg-AMC. Hydrolysis was followed until cathepsin B was completely inactivated (typically 5–30 min). The first-order rate constant for inactivation (k_{obs}) was obtained by non-linear regression of the progress curves using the equation [22,23]:

$$\mathrm{RFU} = \frac{v_i}{k_{obs}}\left(1 - e^{k_{obs}t}\right) + \mathrm{offset}, \tag{1}$$

where RFU represents the relative fluorescence at any time t, v_i is the initial rate before the onset of inhibition, *offset* takes into account a non-zero RFU starting point due to background fluorescence, and k_{obs} is the observed first-order rate constant for inactivation of cathepsin B at a given concentration of inhibitor. The second-order rate constant of inactivation (k_{inact}/K_I) for each inhibitor was determined from the slope of the linear replot of k_{obs} versus inhibitor concentration corrected for substrate competition according to Eq. (2) [24]:

$$k_{obs} = \left(\frac{k_{inact}}{K_I}\right) I \Big/ \left(1 + \frac{S}{K_m}\right). \tag{2}$$

The pK_a values for the ionization events affecting k_{inact}/K_I or k_{cat}/K_m were obtained by fitting the rate constant versus pH data to the appropriate equations as indicated in Section 3 [3,25,26].

3. Results

3.1. pH Activity profiles using the substrate Boc-Leu–Lys–Arg-AMC

The second-order rate constant (k_{cat}/K_m) increases sharply from pH 4 to 6 with a continuing slight increase from pH 6 to 7.8 (Fig. 2). The first ionization event calculated from the pH activity profile (Fig. 2) by use of Eq. (3) (see Model 2 in

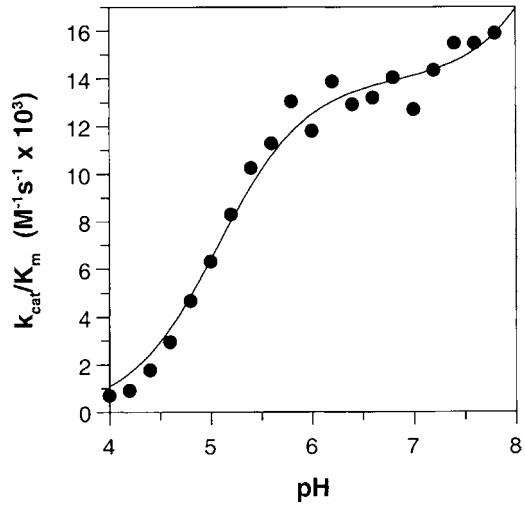

Fig. 2. pH-Dependence of k_{cat}/K_m for the reaction of Boc-Leu–Lys–Arg-AMC with cathepsin B. The solid line represents the best fit to Eq. (3) using the parameters $pK_{a1} = 5.1 \pm 0.1$, $(k_{cat}/K_m)_{limit} = 14,000 \pm 1000\,M^{-1}\,s^{-1}$, and $pK_{a2} = 8.9 \pm 2.5$.

reference [3]) is controlled by a single functional group with a pK_a of 5.1 ± 0.1. The limiting second-order rate constant was calculated to be $14,000 \pm 1000\,M^{-1}\,s^{-1}$. This pK_a determination compares favorably with values reported for Z-Arg–Arg-AMC [3,27] and Z-Arg–Arg-NNap [26,28].

$$k_{cat}/K_m = \frac{(k_{cat}/K_m)_{limit_1}}{1 + 10^{(pK_{a1}-pH)} + 10^{(pH-pK_{a2})}} + \frac{(k_{cat}/K_m)_{limit_2}}{1 + 10^{(pK_{a1}+pK_{a2}-2pH)} + 10^{(pK_{a2}-pH)}}. \quad (3)$$

In other studies using Z-Arg–Arg-AMC as substrate, the second ionization event has been assigned pK_a values of >7.3 and 8.2 with human and rat liver cathepsin B, respectively [3,27]. From our data only an estimate of the pK_a for the second ionization could be made ($pK_a = 8.9 \pm 2.5$).

3.2. pH Profiles of cathepsin B inactivators

The concentration-dependent rate of inactivation (k_{obs}) for the occluding loop binding inactivators APC-5840 and APC-8754 and the primarily non-prime-side-binding inactivators E-64 and APC-3316 over a pH range of 4 to 7.8 in 0.2 pH increments was calculated from progress curves by use of Eq. (1) (Fig. 3). For each inhibitor at every pH, the rate of inactivation was not saturated at the highest concentration of inhibitor employed. Thus, the second-order rate constant of inactivation (k_{inact}/K_I) was calculated from the linear replot of k_{obs} versus inhibitor concentration by use of Eq. (2) (inset Fig. 3). The K_m for Boc-Leu–Lys–Arg-AMC (300 μM) changed very little over this pH range, and an S/K_m ratio of unity was employed for calculations using Eq. (2). The pH dependence of k_{inact}/K_I for both of the occluding loop binding cathepsin B inhibitors (APC-5840 and APC-8754) as well

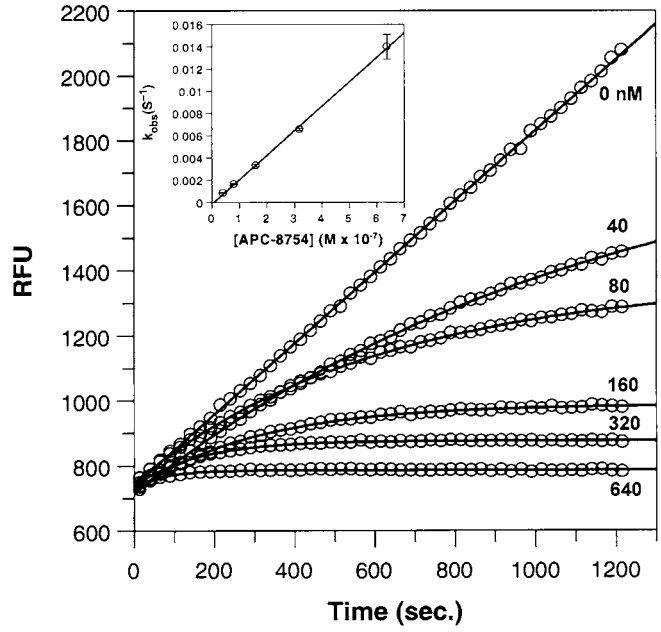

Fig. 3. Kinetics of the inhibition of cathepsin B by APC-8754. Reaction progress curves are shown for the hydrolysis of Boc-Leu–Lys–Arg-AMC (300 μM) at pH 5.8 in assay buffer and in the presence of 0, 40, 80, 160, 320, and 640 nM APC-8754. The reaction was initiated by the addition of 1.1 nM (final) cathepsin B. The lines were drawn according to Eq. (1) (except for the no inhibitor data which was simply fit to a straight line). The inset shows the linear dependence of the rate of reaction with cathepsin B on the concentration of APC-8754. The second-order rate constant for inactivation was determined from the slope of the straight line corrected for substrate concentration by use of Eq. (2).

as for E-64 were very similar (Fig. 4). A sharp drop in the second-order rate of inactivation was observed from pH 4 to 5. The limiting second-order rate of inactivation and pK_a were obtained by fitting the k_{inact}/K_I versus pH data to Eq. 4. For APC-5840 and APC-8754 the inactivation rate approached zero at or above pH 7, while for E-64 the inactivation rate approached a non-zero value (Fig. 4A)

$$k_{inact}/K_I = \frac{(k_{inact}/K_I)_{limit}}{1 + 10^{(pH - pK_a)}}. \quad (4)$$

The pH dependence of k_{inact}/K_I for the non-prime-side directed inhibitor APC-3316 was dramatically different from that of the inhibitors described above (Fig. 5). There was little change observed in the second-order rate of inactivation from pH 4 to 6 followed by a sharp increase up to pH 7.4 (under the conditions employed to assay APC-3316, the rates of inactivation were too fast to accurately measure above pH 7.4). The limiting second-order rate of inactivation was calculated (Eq. (5)) to be $4.2 \times 10^4\,M^{-1}\,s^{-1}$ and was controlled by a single ionizable group with a pK_a of 7.7. The inhibitory activity of APC-3316 was not completely abolished at low pH (Fig. 5)

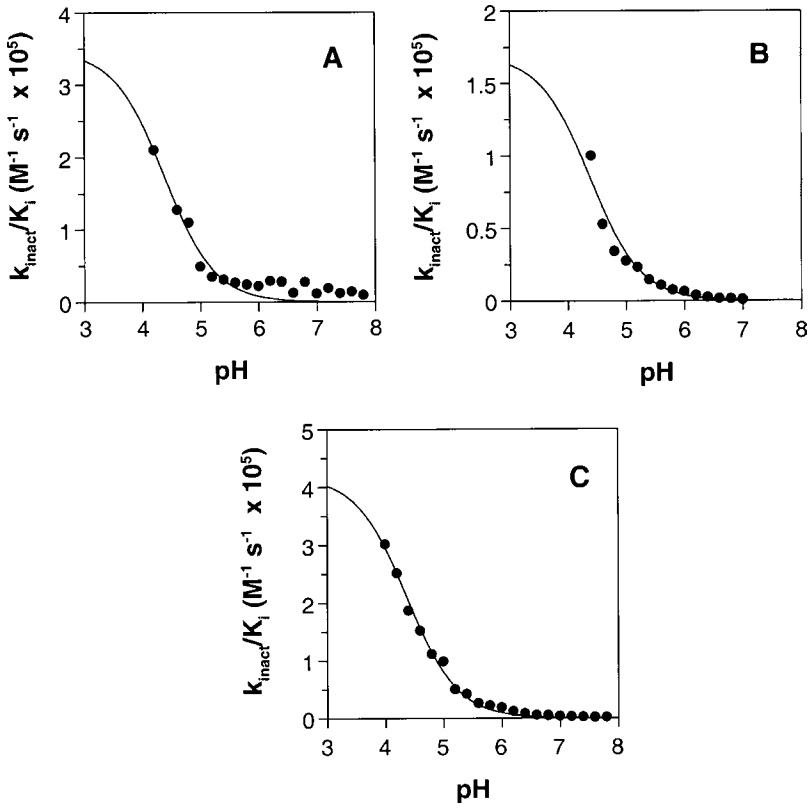

Fig. 4. pH-Dependence of k_{inact}/K_I for the cathepsin B inhibitors E-64 (A), APC-5840 (B), and APC-8754 (C). The lines were drawn according to Eq. (4) using the following fitted parameters: E-64, $pK_a = 4.4 \pm 0.1$, $(k_{inact}/K_I)_{limit} = (3.5 \pm 0.6) \times 10^5\,M^{-1}\,s^{-1}$; APC-5840, pK_a fixed at 4.38, $(k_{inact}/K_I)_{limit} = (1.7 \pm 0.1) \times 10^5\,M^{-1}\,s^{-1}$; APC-8754, $pK_a = 4.37 \pm 0.04$, $(k_{inact}/K_I)_{limit} = (4.2 \pm 0.2) \times 10^5\,M^{-1}\,s^{-1}$.

$$k_{inact}/K_I = \frac{(k_{inact}/K_I)_{limit}}{1 + 10^{(pK_a - pH)}}. \quad (5)$$

4. Discussion

4.1. pH Dependence of non-prime-side-binding substrates and inhibitors

It is known that cathepsin B has a complex pH rate profile and that deletion of the occluding loop has a dramatic effect on the kinetics of substrate hydrolysis [2,3,5–7,27]. Although different substrate and assay conditions were employed in this study, the pH profile for hydrolysis of Boc-Leu–Lys–Arg-AMC is very similar to previous reports (Fig. 2) [3,27]. A large increase in k_{cat}/K_m occurring with a pK_a

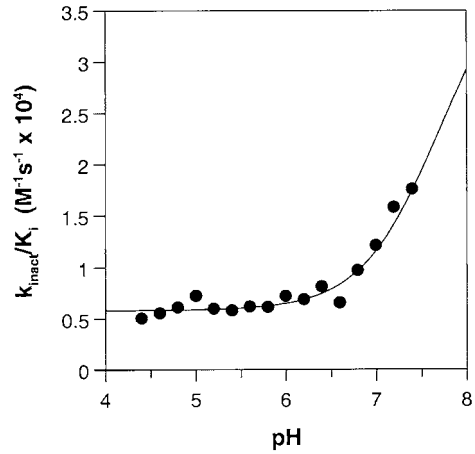

Fig. 5. pH-Dependence of k_{inact}/K_I for the cathepsin B inhibitor APC-3316. The line was drawn according to Eq. (5) using the following fitted parameters: $pK_a = 7.7 \pm 0.2$, $(k_{inact}/K_I)_{limit} = (4.1 \pm 0.9) \times 10^4\,M^{-1}\,s^{-1}$.

of 5.0–5.4 for the commonly used substrate Z-Arg–Arg-AMC has been attributed to the formation of an ionic interaction between the P2 arginine of the substrate and Glu-245 in the S2 pocket of cathepsin B [29,30]. In a hydrophobic environment such as the S2 pocket of cathepsin B, it is reasonable for the carboxylic acid side chain of glutamate to have a slightly elevated pK_a in this range. The substrate Boc-Leu–Lys–Arg-AMC behaves very much like Z-Arg–Arg-AMC in terms of its pH profile (Fig. 2), presumably forming a similar ionic interaction via a P2 lysine. However, for the non-prime-side inactivator APC-3316, the pH profile lacks the same large change in k_{inact}/K_I around pH 5 that is seen with substrates containing a basic residue in the P2 position (Fig. 5). APC-3316 binding is more analogous to that of the substrate Z-Phe–Arg-AMC, wherein a P2 phenylalanine binds the S2 pocket. The binding interaction is still favorable in the large hydrophobic S2 pocket; however, the lack of an ionizable group at P2 of the inhibitor (or substrate) diminishes the importance of deprotonation at Glu-245 [3]. In fact, we have examined the pH dependence of over 40 uncharged, non-prime-side binding, reversible inhibitors and have found that the pattern of inhibition resembles that of APC-3316. Very little change in the apparent K_I is observed from pH 4 to 6 followed by an increase in affinity up to pH 7.4 (data not shown). The rate of inactivation of cathepsin B by APC-3316 is controlled by a single ionizable group with a pK_a of 7.7. The identity of the group responsible for this ionization is not known, but there has been speculation based on differences between analogous pNA and AMC substrates that a residue which lies in the prime-side of the binding cleft of cathepsin B, possibly His 110 or His 111, may be responsible for this pK_a [3]. This seems unlikely in light of structural data, because the occluding loop containing His 110 and His 111 is quite flexible and probably out of the binding cleft at neutral pH [6].

4.2. pH Dependence of occluding loop binding substrates and inhibitors

Originally, the pH-dependent transition from exo- to endo-protease was examined with the exo-substrate Gly–Gly–Phe(NO_2)–Leu [2]. The transition was reported to occur at a pH of approximately 5.5 because of the inflexion in the k_{cat}/K_m versus pH plot. However, at that time the role of the occluding loop was not appreciated, and so it was thought that an ionizable group within the active site cleft might be responsible for the observed transition in protease specificity. Following the elucidation of the crystal structure of both pro-cathepsin B [31] and mature cathepsin B bound by occluding loop binding inhibitors [32], a model involving the location and movement of the occluding loop was invoked to explain the pH-dependent modulation of cathepsin B specificity. From X-ray crystal structures of CA-074 and CA-030 bound to cathepsin B [32], a salt bridge is apparent between His 110 and Asp 24 which anchors the occluding loop down in the active site and positions His 111 optimally at the end of the S2′ pocket to form a salt bridge with the C-terminal carboxylate of either an inhibitor or of an exo-substrate. A second anchoring salt bridge is formed between Arg 116 and Asp 224. Mutagenesis experiments indicate that disrupting either of these two salt bridges dramatically diminishes the pH dependence of inhibition by pro-region peptides [5–7]. Though elegant, the mutagenesis studies lack detailed pH rate data and thus place the transition from exo- to endo-protease in a broad range from pH 4–6. In the present study, analogues of CA-074 were synthesized to probe the feasibility of exploiting occluding loop contacts in the design of potent and selective cathepsin B inhibitors. The strong pH dependence of the inactivation rates is consistent with the hydrogen ion-dependent gating of the occluding loop into either the closed (low pH) or the open (neutral pH) positions. In fact, the pH dependence of the occluding loop binding inhibitors is a direct measure of this gating process. Surprisingly, the pH profile for E-64 mimicked that of the occluding loop binding inactivators APC-5840 and APC-8754. The X-ray crystal structure of E-64 bound to papain and modeling predictions of the binding mode of E-64 to cathepsin B indicate that E-64 binds the non-prime-side of the active site cleft. This orientation does place the free carboxylate group of E-64 onto the prime-side of the active site cysteine, but it is still several angstroms from the occluding loop contacts. Regardless, the results indicate that E-64 binding is affected by increasing pH in a manner similar to that of APC-5840 and APC-8754 (Fig. 4). The major difference in E-64 binding compared with APC-5840 and APC-8754 is the relative independence of the inactivation rate above pH 5.5. At low pH cathepsin B inactivation for all three inhibitors is dominated by an ionic interaction with the terminal carboxylate of the inhibitor and a basic residue on the enzyme, but at a pH above 5.5 this ionic interaction is lost and it appears that for E-64 non-prime side interactions dominate the pH rate profile. Unlike APC-5840 and APC-8754 which make minimal non-prime-side interactions and whose inactivation rates go to zero, E-64 extends much further into the non-prime-side of the active site, and it appears that these interactions are providing enough binding energy to afford measurable inactivation rates at higher pH. The identity of the basic residue interacting with the terminal carboxylates of these inhibitors is presumably His 111. To explain the results with E-64, we believe that the occluding loop may be more flexible than expected or

perhaps modeling results with E-64 bound to cathpesin B do not give a complete picture. Regardless, the decrease in k_{inact}/K_I with increasing pH observed with occluding loop binding inhibitors corresponds to a single ionizable group with a pK_a of 4.4, suggesting that the transition from exo- to endo-protease occurs at pH 4.4 not 5.5, as originally reported [2]. However, both values are within the broad range indicated in more recent studies [5–7]. It is reasonable to assume that the pK_a of this transition is significant for cathespin B-catalyzed processing of proteins targeted for lysosomal degradation, and it should also impact the role of cathepsin B in pathological conditions.

Under normal physiological conditions cathepsin B activity is found predominantly in the lysosomal fraction of cells as opposed to the early endosomal or late endosomal fractions [33]. The pH of mature lysosomes ranges from 4.5 to 5.0 [34,35]. Over this range, and considering that the pK_a of the transition in cathepsin B specificity is 4.4, a mixture of endo- and exo-proteolytic cathepsin B activities should be present with a slightly greater percent active as an endo-protease. Perhaps this is an efficient mix to afford more complete proteolytic digestion. In a pathological state such as tumor invasion, cathepsin B is found outside the lysosomal compartment [8,13,14,36–38], and inhibitors specifically designed to target occluding loop contacts will be strongly dependent on the pH of the specific cellular compartment or physiological milieu in which cathepsin B is active. The results presented herein imply that targeting the occluding loop of cathepsin B may be a poor inhibitor design strategy if the enzyme environment has a pH greater than 5.5. However, highly selective, occluding loop binding inhibitors effective at preventing or slowing metastasis would shed light not only on the physical environment in and around invading tumor cells but also on the role cathepsin B plays in tumor invasion. Such inhibitors could potentially be useful chemotherapeutic agents.

Acknowledgments

The authors would like to thank K. Elrod and J. Janc for critically reading the manuscript and J. McCarter for help in interpreting and communicating the results.

References

[1] L. Mach, J. Mort, J. Glossl, J. Biol. Chem. 269 (1994) 13030–13035.
[2] L. Polgar, C. Csoma, J. Biol. Chem. 262 (1987) 14448–14453.
[3] H. Khouri, C. Plouffe, S. Hasnain, T. Hirama, A. Storer, R. Menard, Biochem. J. 275 (1991) 751–757.
[4] D. Musil, D. Zucic, D. Turk, R. Engh, I. Mayr, R. Huber, T. Popovic, V. Turk, T. Towatari, N. Katunuma, et al., EMBO J. 10 (1991) 2321–2330.
[5] C. Illy, O. Quraishi, J. Wang, E. Purisima, T. Vernet, J. Mort, J. Biol. Chem. 272 (1997) 1197–1202.
[6] D. Nagler, A. Storer, F. Portaro, E. Carmona, L. Juliano, R. Menard, Biochemistry 36 (1997) 12608–12615.

[7] O. Quraishi, D. Nagler, T. Fox, J. Sivaraman, M. Cygler, J. Mort, A. Storer, Biochemistry 38 (1999) 5017–5023.
[8] J. Mai, D.M. Waisman, B.F. Sloane, Biochim. Biophys. Acta 1477 (2000) 215–230.
[9] B. Sloane, J. Rozhin, T. Lah, N. Day, M. Buck, R. Ryan, J. Crissman, K. Honn, Adv. Exp. Med. Biol. 233 (1988) 259–268.
[10] B. Sloane, J. Rozhin, D. Robinson, K. Honn, Biol. Chem. Hoppe Seyler 371 (Suppl.) (1990) 193–198.
[11] J.L. Cox, P.S. Sexton, T.J. Green, N.A. Darmani, Melanoma Res. 9 (1999) 369–374.
[12] S. Michaud, B.J. Gour, Exp. Opin. Ther. Patents 8 (1998) 645–672.
[13] S. Yan, M. Sameni, B. Sloane, Biol. Chem. 379 (1998) 113–123.
[14] D. Keppler, M. Sameni, K. Moin, T. Mikkelsen, C. Diglio, B. Sloane, Biochem. Cell Biol. 74 (1996) 799–810.
[15] T. Towatori, T. Nikawa, M. Murata, C. Yokoo, M. Tamai, K. Hanada, N. Katunuma, FEBS Lett. 280 (1991) 311–315.
[16] M. Murata, S. Miyashita, C. Yokoo, M. Tamai, K. Hanada, K. Hatayama, T. Towatori, T. Nikawa, N. Katunuma, FEBS Lett. 280 (1991) 307–310.
[17] B. Linebaugh, M. Sameni, N. Day, B. Sloane, D. Keppler, Eur. J. Biochem. 264 (1999) 100–109.
[18] N. Schaschke, I. Assfalg-Machleidt, W. Machleidt, D. Turk, L. Moroder, Bioorg. Med. Chem. 5 (1997) 1789–1797.
[19] B. Gour-Salin, P. Lachance, C. Plouffe, A. Storer, R. Menard, J. Med. Chem. 36 (1993) 720–725.
[20] J.S. Nowick, N.A. Powell, T.M. Nguyen, G. Noronha, J. Org. Chem. 57 (1992) 7364–7366.
[21] J.T. Palmer, D. Rasnick, J.L. Klaus, D. Bromme, J. Med. Chem. 38 (1995) 3193–3196.
[22] S. Cha, Biochem. J. 24 (1975) 2177–2185.
[23] J.F. Morrison, C.T. Walsh, in: A. Meister (Ed.), Advances in Enzymology and Related Areas of Molecular Biology, Wiley, New York, 1988, pp. 201–301.
[24] S.R. Stone, J. Hofsteenge, Biochemistry 25 (1986) 4622–4628.
[25] W.W. Cleland, Methods Enzymol. 87 (1982) 390–405.
[26] F. Willenbrock, K. Brocklehurst, Biochem. J. 227 (1985) 521–528.
[27] S. Hasnain, T. Hirama, A. Tam, J. Mort, J. Biol. Chem. 267 (1992) 4713–4721.
[28] F. Willenbrock, K. Brocklehurst, Biochem. J. 222 (1984) 805–814.
[29] S. Hasnain, T. Hirama, C. Huber, P. Mason, J. Mort, J. Biol. Chem. 268 (1993) 235–240.
[30] Z. Jia, S. Hasnain, T. Hirama, X. Lee, J. Mort, R. To, C. Huber, J. Biol. Chem. 270 (1995) 5527–5533.
[31] D. Turk, M. Podobnik, R. Kuhelj, M. Dolinar, V. Turk, FEBS Lett. 384 (1996) 211–214.
[32] D. Turk, M. Podobnik, T. Popovic, N. Katunuma, W. Bode, R. Huber, V. Turk, Biochemistry 34 (1995) 4791–4797.
[33] V. Claus, A. Jahraus, T. Tjelle, T. Berg, H. Kirschke, H. Faulstich, G. Griffiths, J. Biol. Chem. 273 (1998) 9842–9851.
[34] S. Ohkuma, B. Poole, Proc. Natl. Acad. Sci. USA 75 (1978) 3327–3331.
[35] M.J. Geisow, Exp. Cell Res. 150 (1984) 29–35.
[36] E. Elliott, B.F. Sloane, Perspect. Drug Discovery Des. 6 (1996) 12–32.
[37] K. Moin, L. Cao, N. Day, J. Koblinski, B. Sloane, Biol. Chem. 379 (1998) 1093–1099.
[38] J. Rozhin, M. Sameni, G. Ziegler, B. Sloane, Cancer Res. 54 (1994) 6517–6525.